Algal Research 90 (2025) 104146

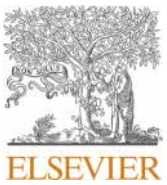

Contents lists available at ScienceDirect

Algal Research

journal homepage: www.elsevier.com/locate/algal

Short communication

The metabolome of crustose coralline algae is driven by phylogeny and environmental conditions

Camille Vizon [a,*], Laura Lagourgue [b], Hendrikje Jorissen [a,c], Delphine Raviglione [a,d], Claude E. Payri [b], Isabelle Bonnard [a,d], Maggy M. Nugues [a,e]

[a] PSL Université Paris: EPHE-CNRS-UPVD, UAR 3278 CRIOBE, Université de Perpignan, 66860 Perpignan, France
[b] UMR 9220 ENTROPIE 'Ecologie Marine Tropicale des Océans Pacifique et Indien' (IRD-CNRS- Université de Nouvelle-Calédonie – Université de La Réunion), IRD, 98848 Nouméa, New Caledonia
[c] Hawai'i Institute of Marine Biology, University of Hawai'i at Mānoa, Hawai'i, Kāne'ohe, USA
[d] Plateau technique MSXM, plateforme Bio2Mar, Université de Perpignan via Domitia, Perpignan Cedex 9, France
[e] Laboratoire d'Excellence Corail, 66860 Perpignan, France

ARTICLE INFO

Keywords:
Crustose coralline algae
Extraction method
Metabolomics
Reef habitat
Microhabitat
Phylogeny

ABSTRACT

Metabolomics is a powerful approach to investigate the effect of environmental conditions on metabolite variations in marine algae. Here, we focused on crustose coralline algae (CCA), a group of calcifying, red algae which play an important role on coral reefs through their interactions with corals and contribution to coral reef formation. Despite their ecological importance, little is known about their metabolome and how it varies with environmental conditions and phylogeny. Using an untargeted metabolomic approach, we explored the metabolomic fingerprints of seven CCA species (order: Corallinales) commonly found on the coral reefs of Moorea, French Polynesia. We developed an extraction method to characterize the CCA metabolome on two sample types (whole fragment and surface only) and explored the chemical variations of CCA across species, reef habitat and microhabitat. The extraction method successfully characterized the CCA metabolome, as demonstrated by a technical variability lower than the biological variability for both sample types. The CCA metabolome was species-specific and a correlation was found between phylogenetic taxonomy and metabolomic profiles of the different species. Moreover, the metabolomic composition of certain species differed between the back and fore reef habitats and between exposed and cryptic microhabitats. These results highlight a high variability in the CCA metabolome mediated by phylogeny and environmental conditions. This study provides valuable insights into the sources of metabolomic variation in CCA. It lays the groundwork for exploring the ecological functions of the CCA metabolome and its potential use as a tool to assess organismal and ecosystem health.

1. Introduction

Marine organisms produce a wide range of secondary metabolites that have different ecological functions. These secondary metabolites are the end products of biological processes and are defined as small molecules of low molecular weight [1]. Recent advances in metabolomics have enabled to describe these metabolites and how their diversity and composition vary under different environmental conditions at a given time [2]. This approach requires a high degree of robustness and reproducibility as interpretation can change according to extraction or analytical methods [3,4]. Additionally, metabolomics is a powerful tool to evaluate the effect of environmental factors on living organisms, particularly marine algae [4–6]. For example, it has been used to discriminate between green, red and brown algae [7] and to investigate the effects of different factors on metabolite variability in several algal species [8,9].

Multiple sources of fluctuation have been identified in the metabolome composition of marine organisms, including sponges [10,11], corals [12] and algae [7]. Among these factors, genetic and environmental conditions have emerged as predominant drivers of metabolome variation [13,14]. For instance, differences in the metabolome of green, red and brown seaweeds mirror host phylogeny [13,15]. Marine algae

* Corresponding author.
E-mail address: camille.vi@hotmail.fr (C. Vizon).

https://doi.org/10.1016/j.algal.2025.104146
Received 22 April 2025; Received in revised form 10 June 2025; Accepted 13 June 2025
Available online 14 June 2025

can adapt to highly changing environments and modulate the biosynthesis of secondary (specialized) metabolites according to environmental conditions [9,16]. Their chemical composition can be influenced by a number of environmental and biological parameters, such as temperature [17], salinity [18], light intensity [19], nutrient availability [19], herbivory [16], species [13], life history stage [8] and lifestyle [20]. Their habitat can also influence their metabolome [4,6]. Spatiotemporal metabolome variations have been observed in different algal species, such as *Asparagopsis taxiformis* [6,9] and algae of the *Lobophora* genus [4,21].

Here, we focused on crustose coralline algae (CCA). These red calcareous algae belong to the orders Corallinales, Corallinapetrales, Hapalidiales and Sporolithales and are common in the euphotic zone of many marine benthic habitats [22,23]. On coral reefs, they contribute to reef formation and primary productivity [24], act as settlement inducer for coral larvae [25], and inhibit the recruitment of macroalgae that could otherwise harm corals [26]. Despite their ecological importance, few studies have investigated the sources of metabolomic variation in CCA species. CCA are complex holobionts with a diverse microbiome [27] and metabolome [30]. Investigations on their chemical ecology have led to significant advances in areas such as the composition of their dissolved organic matter exudates [28], signaling compounds and/or microbes underpinning coral recruitment [20], and allelopathic activity against algal spores [29]. However, the CCA metabolome and its environmental and genetic variability remain largely understudied.

The goal of this study was to reveal the variation patterns of CCA metabolomes and how these variations are influenced by environmental conditions and phylogeny using an untargeted metabolomic approach. Specifically, we aimed: i) to develop an extraction method to characterize the CCA metabolome and ii) to describe the variation patterns in the CCA metabolome across species, reef habitats and microhabitats. We targeted 7 CCA species distributed across a range of reef habitats and microhabitats on the coral reefs of Moorea, French Polynesia. Species identification was based on morphological observations and genetic characterization. Since algal metabolome varies with species [20,30] and environmental conditions [4], we hypothesized that the CCA metabolome would vary according to phylogeny, reef habitats and microhabitats.

2. Materials and methods

2.1. Study site and species

We studied the CCA metabolome at 2 sites (17° 28′ 52.7" S, 149° 50′ 55.62"W and 17° 28′ 47.2" S, 149° 51′ 06.8" W) representing 2 reef habitats (back reef and fore reef, respectively). The seabed on the back reef was characterized by scattered massive *Porites* colonies, interspersed with sand and rubble, and colonized by macroalgae, branching corals, and turf. The fore reef consisted of low relief coral spur-and-groove formations, primarily covered by branching *Pocillopora* colonies, CCA and turf. The back reef was subject to high light intensity and nutrient loading, while the fore reef was low in light intensity and nutrient and experienced intense fish grazing [31,32]. Both habitats exhibited a high diversity of CCA species.

We studied 7 CCA species or species complex (thereafter simply referred to as 'species'): *Dawsoniolithon* spp. (family: Porolithaceae), *Harveylithon minutum* (Porolithaceae), *Porolithon* cf. *onkodes* (Porolithaceae), *Hydrolithon* spp. (Hydrolithaceae), *Lithophyllum flavescens* (Lithophyllaceae), *Lithophyllum insipidum* (Lithophyllaceae) and *Neogoniolithon* cf. *megalocystum* (Spongitidaceae) (Fig. S1). These species were selected because they are commonly found on the coral reefs of Moorea and can be reliably identified in-situ [33,34]. CCA samples were identified based on morphological observations in the field and laboratory by the same observer (MN), as well as DNA analyses on 60 samples collected in September 2021 (Table S1). Four genes were targeted for DNA-based analyses: the chloroplast gene *psb*A, the mitochondrial cytochrome *c* oxidase subunit 1 (COI) gene and the two rDNAs SSU (small subunit or 18S) and LSU (large subunit, or 28S). Total DNA extraction and genes amplification followed protocols used by Caragnano et al. [35]. PCR products were sequenced by Genoscreen (Lille, France).

2.2. Metabolomic signatures of CCA species

2.2.1. Sampling

CCA fragments (ca. 10–15 cm^2) were collected using hammer and chisel in April 2016. To validate the extraction method, fragments ($n = 10$) of *Hydrolithon* spp. and *P.* cf. *onkodes* were collected at the back reef at 1–2 m depth. Each replicate fragment was selected from a haphazardly chosen individual patch. For interspecies comparison, fragments ($n = 5$) of all 7 CCA species were collected from the same back reef site. For inter-habitat comparison, fragments (n = 5) of 5 CCA species (*Hydrolithon* spp., *L. insipidum*, *N.* cf. *megalocystum*, *Dawsoniolithon* spp., and *P.* cf. *onkodes*) were collected from the fore reef at 12–14 m depth and compared with samples from the back reef. For inter-microhabitat comparison, two CCA species (*Hydrolithon* spp. and *P.* cf. *onkodes*) and two microhabitats (exposed vs cryptic) were selected from the back reef site. We defined the exposed microhabitat as an area receiving direct sunlight and easily accessible from grazers, and the cryptic microhabitat as an area low in light intensity and relatively protected from grazers [34]. Since *Hydrolithon* spp. commonly forms rhodoliths (i.e., unattached nodules), *Hydrolithon* spp. rhodoliths ($n = 5$) were sampled. Exposed and cryptic samples were collected from their top and bottom surfaces, respectively. Note that, for the previous comparisons, only the top (i.e., exposed) surfaces of *Hydrolithon* spp. rhodoliths were sampled. For *P.* cf. *onkodes*, it was not possible to find individuals subject to both microhabitats. Thus, samples ($n = 5$) were collected from haphazardly chosen individuals in each microhabitat. Fragments were placed in a separate Ziplock bag filled with seawater and transported in a closed cooler to the CRIOBE research station. In the laboratory, samples were immediately frozen at −20 °C, freeze-dried and stored at −20 °C until chemical extraction to preserve the integrity of biological samples [36].

2.2.2. Metabolites extraction

The validation of the extraction method was performed on two sample types: i) whole CCA fragment, and ii) CCA surface only ($n = 5$ for each type). Whole fragment biological replicates (250 mg) were obtained by grinding fragments with a mortar and pestle, while surface biological samples (250 mg) were obtained by scrapping the living CCA surface with a scalpel. To obtain technical replicates, additional powder (250 mg) was obtained from each fragment by further grinding or scrapping as appropriate. The resulting powder was pooled across sample types, homogenized and divided in 5 equal samples. Sufficient additional powder could not be obtained from *P.* cf. *onkodes* surface samples, thus technical replicates could not be performed for these samples. For comparisons across species, habitats and microhabitats, CCA surface biological samples were processed. For all samples, a biphasic solid-liquid extraction was performed with a mixture of methyl ter-butyl ether (MTBE), methanol (MeOH) and ultrapure water (*v*/v/v, 7:3:1). Algae powder was first extracted with a mixture of MTBE and MeOH under 5 min of vortex and sonification. Then, ultrapure water was added and the entire extract was vortexed and extracted under sonification. The mixture was centrifuged at 2050*g* for 20 min to obtain two phases and the organic phase was carefully transferred into glass tube. The extraction was carried out three times, and extracts were pooled and evaporated using a Genevac TM centrifugal concentrator (EC-2 series, SP Industrie, UK).

2.3. Mass spectrometry analysis and data processing

2.3.1. Analytical system

Samples were resolubilized in MeOH, prepared at 1 mg mL^{-1} and

filtrated on Uptidisk (PTFE, 13 mm, 0.2 μm, Interchim, San Diego, California). Quality Control (QC) samples were prepared by pooling equal volume of each sample to ensure reproducibility and absence of analytical drift (Fig. S2). Samples were injected over two analytical sequences and run under the same analytical conditions. The first sequence included samples for the method validation, while the second sequence included samples for the inter-species, habitats and microhabitats comparisons. For both sequences, MeOH blanks and QC samples were injected at the beginning to ensure system suitability and column condition. QC samples were injected every 7 samples to detect analytical drift.

All samples were injected in HPLC-MS using an Accela system (autosampler and quaternary pump), coupled with a LCQ Fleet ion trap from Thermo Scientific (Waltham, Massachussetts), equipped with an electrospray ion source. The separation was achieved using a Kinetex C6-phenyl column (1.7 μm, 100 Å, 100 × 2.1 mm, Phenomenex, Torrance, CA, USA) at 30 °C with a flow rate of 270 μL min^{-1}. Gradient solvents were composed of H_2O + 0.1 % formic acid (A) and acetonitrile +0.1 % of formic acid (B). The gradient system was programmed as follows: 60 % of (B) for 2 min, from 60 % to 80 % (B) in 6 min, from 80 % to 100 % (B) in 14 min, 100 % (B) for 6 min, from 100 % to 60 % (B) in 2 min, and 60 % (B) for 8 min (38 min/run). For MS conditions, ionization was operated in positive ion mode. Sheath gas flow rate was set to 25 a.u (arbitrary units), auxiliary gas was set to 5 a.u and sweep gas was set to 1 a.u. The capillary temperature was set to 290 °C, and a spray-voltage of 4.5 kV was applied. The source current was set to 100 UA with a tube lens of 120 V. The analysis was acquired in a full scan mode between a mass range of 150 to 2000 *m/z*.

2.3.2. Mass spectral data processing

Raw HPLC-MS data were converted to mzXML files in centroid mode using MS convert software (version 3.0, from Proteowizard library, Palo Alto, CA, USA). mzXML files from each analytical sequence were loaded and processed separately using Workflow4Metabolomics on the Galaxy web platform [37]. Optimized parameters were set as follows: a peak picking (method = "MatchedFilter", binSize = 0.2, steps = 2, mzdiff = 0.4, sntresh = 30 for the first sequence and 10 for the second sequence), a peak grouping (bw = 30, minfrac = 0.2, minSize = 0.25), a correction of retention time (method = "obiwarp"), a matching peak across samples (bw = 10, minfrac = 0.2, minSize = 0.25), a peak filling and a 'CAMERA' peak annotation. Two feature tables with features *m/z*, retention time and peak intensity were generated from each sequence. These included 482 and 937 features, respectively. A first filtration step was applied by removing features whose intensity was higher than in MeOH blanks (t-stat, $p < 0.05$). A second filtration was applied by removing features whose relative area was upper than 30 % of the pooled QC samples. Since the QCs of each sequence were well superimposed in the PCA, a batch correction was not applied in either dataset. Finally, redundancies due to isotopes were manually removed and only monoisotopic mass were kept. Final feature tables for the two sequences included 326 and 378 features, respectively. A sum normalization and an auto-scaling were applied to both datasets using MetaboAnalyst 6.0 [38], and datasets were independently analyzed.

2.4. Statistical analysis

Statistical analyses were performed using R (version 4.2.2). Plots were drawn using the *ggplot* package [39]. Differences in metabolomic composition were visualized using a Principal Component Analysis (PCA) with the *vegan* package [40] and analyzed using a Permutational Multivariate Analysis of Variance (PERMANOVA) with the *adonis* function of the same package. Pairwise comparisons were performed using the *pairwise.adonis* function of the *pairwiseAdonis* package and adjusted with the Benjamini and Hochberg method [41]. For the method validation, metabolomic beta-dispersion was calculated using the *betadisper* function and analyzed for each CCA species separately using a one- or two-way Analysis of Variance (ANOVA) (*rstatix* package), including the factors sample type (whole fragment vs surface) and/or replicate type (biological vs technical) as appropriate. For comparisons across species, reef habitats and microhabitats, metabolomic alpha-diversity (Shannon index) and composition were analyzed using parametric ANOVA and PERMANOVA, respectively, with the factors species, species and habitat, and species and microhabitat as appropriate, followed by Tukey's HSD pairwise comparisons. Prior to all ANOVAs, parametric assumptions were tested for normality (Shapiro-Wilk test) and variance homogeneity (Levene's test).

To test the correlation between the DNA and metabolomic profiles of the 7 CCA species, genetic sequences were cleaned, edited in Geneious version 7.1.9 (http://www.geneious.com, [42]) and aligned using the MUSCLE algorithm available in the software. Sequences were then assigned to species with the Basic Local Alignment Search Tool (BLAST; https://blast.ncbi.nlm.nih.gov/, [43]). The genetic distance matrix was compiled with one representative value per species for statistical analysis. Multilocus (*psb*A, COI, SSU, LSU) concatenated matrices were assembled for phylogenetic reconstruction. Maximum likelihood (ML) trees were performed using RAxML [44] through the CIPRES web portal [45] and launched using the "rapid bootstrapping and search for the best-scoring ML tree" algorithm, the GTR + I + G evolutionary model, and 1000 bootstrap (bs) iterations [46]. Results were visualized in Figtree v.1.4.4 [47]. For metabolomic data, clustering was constructed based on mean features per species. The hierarchical clustering analysis (HCA) was then constructed using Euclidean distances and Ward's minimum variance method. The correlation between phylogenetic and metabolomic distance matrix was assessed using a mantel test with the *mantel* function of the *vegan* package.

3. Results and discussion

A total of 73 new sequences were submitted to GenBank, including 12 COI sequences (under accession numbers PV221098-PV221103), 19 p*sbA* sequences (PV174085-PV174103), 21 18S sequences (PV174043-PV174063) and 21 28S sequences (PV174064-PV174084) (Table S1). Genetic analysis allowed us to identify 12 species among our samples and confirmed most of morphological-based assignation: *Dawsoniolithon conicum*, *D.* sp1–4, *Harveylithon minutum*, *Hydrolithon reinboldii*, *H.* sp1, *Lithophyllum insipidum*, *L. flavescens*, *Neogoniolithon* cf. *megalocystum* and *P.* cf. *onkodes*. The distinct species within the genera *Dawsoniolithon* and *Hydrolithon* could not be recognized using morphological observations. Therefore, we used the plural form 'spp.'. Detailed explanations for the suffix 'cf.' in *N.* cf. *megalocystum* and *P.* cf. *onkodes* are provided in Vizon et al. [34].

The extraction method was successful in characterizing the CCA metabolome, as shown by a technical variability lower than the biological variability for both sample types in *Hydrolithon* spp. and for *P.* cf. *onkodes* whole fragments (beta-dispersion: ANOVA: $p < 0.001$ for *Hydrolithon* spp. and $p = 0.004$ for *P.* cf. *onkodes* whole fragment; Table S2; Fig. 1B). This result validates its potential application for CCA metabolomics studies. Not surprisingly, metabolomic composition differed whether sampling whole fragment or surface only (PERMANOVA, $p = 0.001$ for *Hydrolithon* spp. and $p = 0.006$ *P.* cf. *onkodes* biological replicates, Fig. 1A). This difference could be explained by the fact that the biological matrix is a major factor influencing metabolite composition. Marine algae host a wide range of microorganisms, including epi- and endosymbiotic procaryotes and eucaryotes [48,49]. Likewise, CCA host a multitude of specific and distinct microorganisms on their surface [50,51], while their calcareous skeleton is colonized by a wide variety of endolithic communities [52,53]. Therefore, the choice of sample type (i.e., whole fragment vs surface) needs to be carefully considered, notably with regards to research objectives. For example, since this study was part of a wider aim to investigate CCA-associated settlement cues for coral larvae [20], surface samples were processed for the subsequent comparisons.

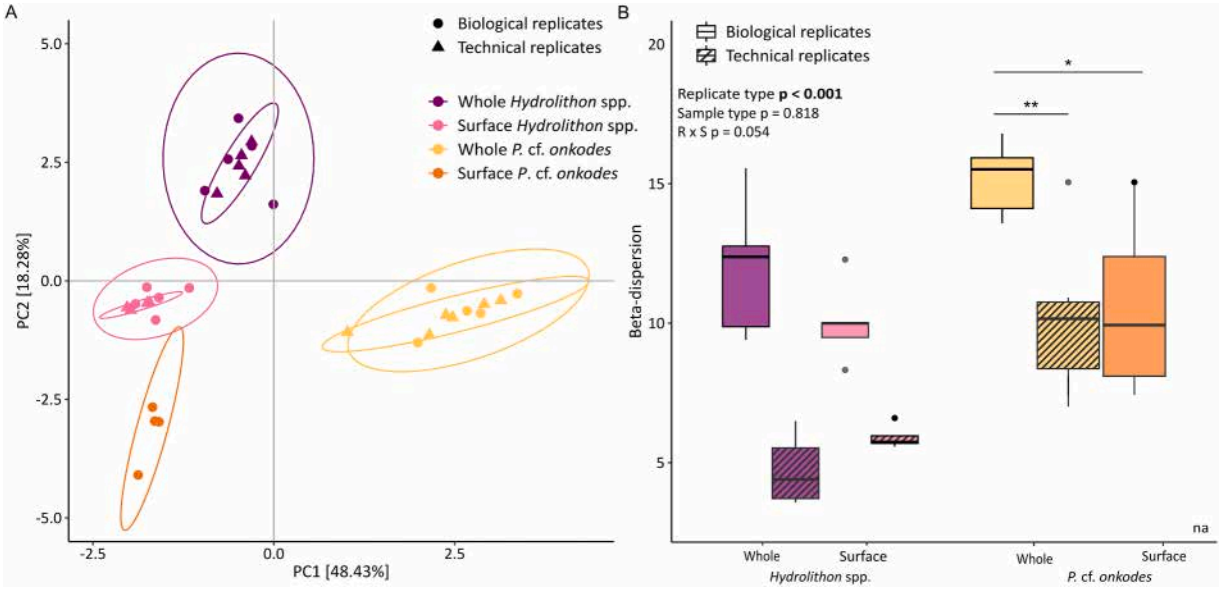

Fig. 1. Effects of replicate types (biological vs technical) and sample types (whole fragment vs surface) on the metabolomic composition (A) and beta-dispersion (B) of *Hydrolithon* spp. and *P.* cf. *onkodes* samples. $n = 5$ for each sample types (whole fragment and surface) and replicates types (biological and technical). Note the absence of technical replicates for the surface *P.* cf. *onkodes* samples (na = not available). Beta-dispersion was analyzed by one- or two-way ANOVAs as appropriate (* $p < 0.05$, ** $p < 0.01$). See supplementary table 2 for detailed analyses and statistical results. Ellipses are 95 % data ellipses. R: Replicate type, S: Sample type.

The CCA metabolome differed both in terms of diversity and composition between the 7 species collected from the back reef (alpha-diversity: ANOVA, $p < 0.001$, Table S3A, Fig. 2A; composition: PERMANOVA, $p = 0.001$, Table S3B, Fig. 2B). These results are consistent with an earlier study on the CCA metabolome in Moorea [20]. Interspecies metabolome variability has been previously observed in marine algae [6,15]. Since these differences could be associated with phylogeny [13], we explored the relationship between phylogenetic taxonomy and metabolomic profiles of the 7 CCA species. The concatenated multilocus phylogeny (Fig. 3) showed that the 7 CCA species were strongly supported (bs = 100), as well as interspecies relationships (bs > 90), except between *Dawsoniolithon* spp. and *H. minutum* (bs = 77). There was a significant correlation between phylogenic and metabolomic distances (Mantel test: $r = 0.54$, $p = 0.028$). The Porolithaceae species were clearly clustered together and presented more related metabolomic profiles than with species from other families. Phylogenetic and metabolomic linkages have been previously reported in birds [54], plants [55] or phytoplankton [14]. In marine algae, metabolomic variabilities between different red, brown and green seaweeds were also consistent with their genetic classification [13]. This correlation supports a co-evolution between DNA and metabolomic profiles and the potential of the metabolomic approach to discriminate between CCA species and follow their evolutionary history.

Nevertheless, some mismatches occurred in the correlation between the DNA and metabolomic profiles. Among the Porolithaceae, *P.* cf. *onkodes* and *Dawsoniolithon* spp. were more closely related based on metabolomic profiles (Fig. 3B), whereas *Dawsoniolithon* spp. was genetically closer to *H. minutum*, but with weak support (Fig. 3A). For the Lithophyllaceae, metabolomic results did not recover the close phylogenetic relationship of the two sister species *L. insipidum* and *L. flavescens*. *L. insipidum* appeared more similar to *H. minutum*, *Dawsoniolithon* spp. and *P.* cf. *onkodes* than to *L. flavescens* in the metabolome-based clustering. Finally, *Hydrolithon* spp. was phylogenetically more related to the two *Lithophyllum* species, while its metabolomic profile was more similar to *N.* cf. *megalocystum*. The moderate correlation between phylogeny and metabolome could also be explained by potentially confounding factors, including but more limited to the CCA associated microbial communities, their physiological status or the presence of boring invertebrates, which could have contributed to the plasticity of the CCA metabolome, but which were not assessed. Additionally, one limitation of this study was that genetic and metabolomic analyses were not conducted on the same samples. Future studies should aim to overcome these shortcomings.

Spatially, the CCA metabolome did not show clear differences across habitats or microhabitats in term of alpha diversity (Tables S4A & S5A; Fig. 2C & E). There was an interaction between species and habitat on metabolomic alpha-diversity (ANOVA, $p = 0.011$), but pairwise comparisons were not significant (Tukey's comparisons: $p > 0.05$; Table S4A). In contrast, metabolomic composition differed across habitats and microhabitats depending on species, as indicated by significant interactions species x habitat and species x microhabitat (PERMANOVA, $p < 0.05$; Tables S4B & S5B; Fig. 2D & F). Post-hoc tests on the metabolomic composition of each species indicated significant differences between back and fore reef habitats for *L. insipidum*, *N.* cf. *megalocystum* and *P.* cf. *onkodes* (Benjamini-Hochberg adjusted pairwise comparisons: $p < 0.05$, Table S4B), as well as a significant difference between exposed and cryptic microhabitats for *Hydrolithon* spp. ($p = 0.006$, Table S5B).

Metabolomic variation has been previously observed at multiple spatial scales in several benthic organisms, including sponges [10,11], corals [12] and marine algae [4,6,9,21]. For example, the metabolome of the red alga *Asparagopsis taxiformis* vary from temperate to tropical regions [6,9]. Likewise, several algal species from the genus *Lobophora* showed metabolomic variation between different reef sites in New-Caledonia [4]. Metabolomic fluctuations in marine algae may be explained by abiotic and biotic factors, such as temperature [17], light intensity [19], nutrient availability [19] and predation [16]. Although not quantified in this study, herbivore pressure, nutrient concentrations, light intensity and UV radiation may be possible sources of spatial metabolomic variations in CCA. In Moorea, light intensity is higher in the back reef than in the fore reef, with means of 446.28 ± 20.99 (SEM) and 137.50 ± 6.82 μmol photons m^{-2} s^{-1}, respectively [32]. Moreover, the fore reef exhibits a higher herbivore pressure and a lower nutrient availability than the back reef [31]. Likewise, the exposed microhabitat is characterized by a high exposure to light and grazers, whereas the cryptic microhabitat is low in light intensity and relatively protected from grazers [33].

Herbivore pressure, nutrient concentrations and light intensity typically regulate the abundance and growth of competitive algae, such

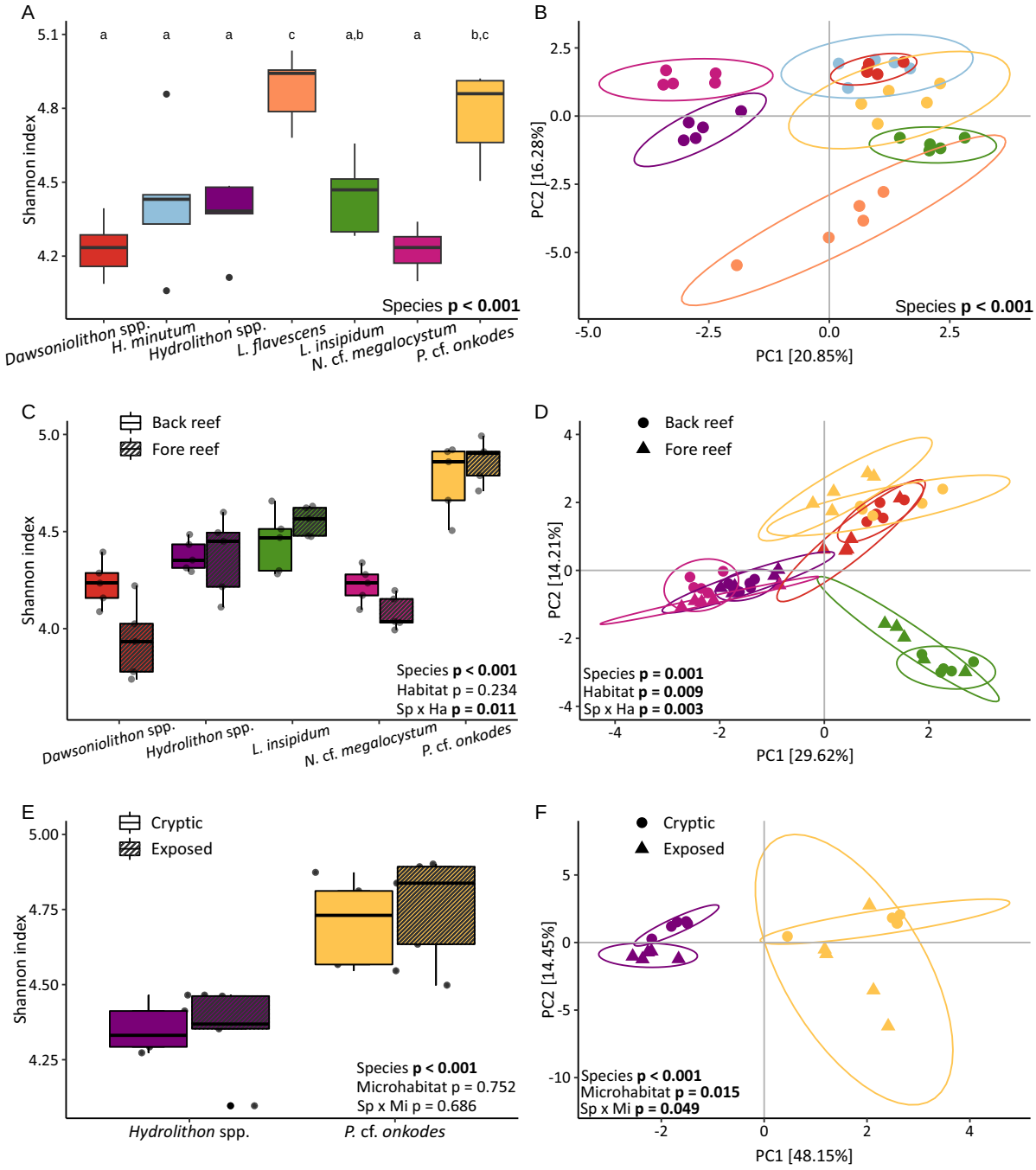

Fig. 2. Effects of species (A-B), reef habitats (back reef vs fore reef) (C—D) and microhabitats (exposed vs cryptic) (*E*-F) on the metabolomic alpha-diversity (Shannon index) (left panels) and composition (right panels) of CCA samples. Shannon diversity data were analyzed by parametric ANOVAs, followed by Tukey post hoc comparisons as appropriate. Metabolomic composition was analyzed by PERMANOVAs. See supplementary tables 3 to 5 for detailed analyses and statistical results. Note that color codes in panels B, D and F correspond to color codes used in panels A, C and E, respectively. Ellipses are 95 % data ellipses. Sp: Species, Ha: Habitat, Mi: Microhabitat. For each comparison, n = 5 replicates per species.

as large canopy macroalgae or algal turfs, which may overgrow and shade CCA, or increase their sediment load by sediment trapping [22,56]. In Moorea, the occurrence of epiphytes on *P.* cf. *onkodes* and *N.* cf. *megalocystum* was found to be higher on the back reef than on the fore reef [34]. This trend was coupled with reduced marginal growth rates on the back reef compared to the fore reef in both species, highlighting the importance of competition with benthic algae on CCA fitness. Likewise, competitive interactions with algae may alter the metabolome of CCA, as previously shown for corals [57]. In addition, benthic organisms, such as sponges and marine algae, can modulate the biosynthesis of their metabolites in response to UV radiation [4,10]. A weak light intensity may lead to a decrease in photosynthesis efficiency, while a high light intensity can cause an oxidative stress [4]. Therefore, marine algae may synthesize metabolites that protect against UV radiation, such as carotenoids pigments or mycosporines like-amino acids [9]. Clearly, further experimental studies should investigate the separate and combined effects of these different factors on the CCA metabolome to allow a full understanding of the sources of its variability.

4. Conclusion

This study demonstrated the application of an extraction method for

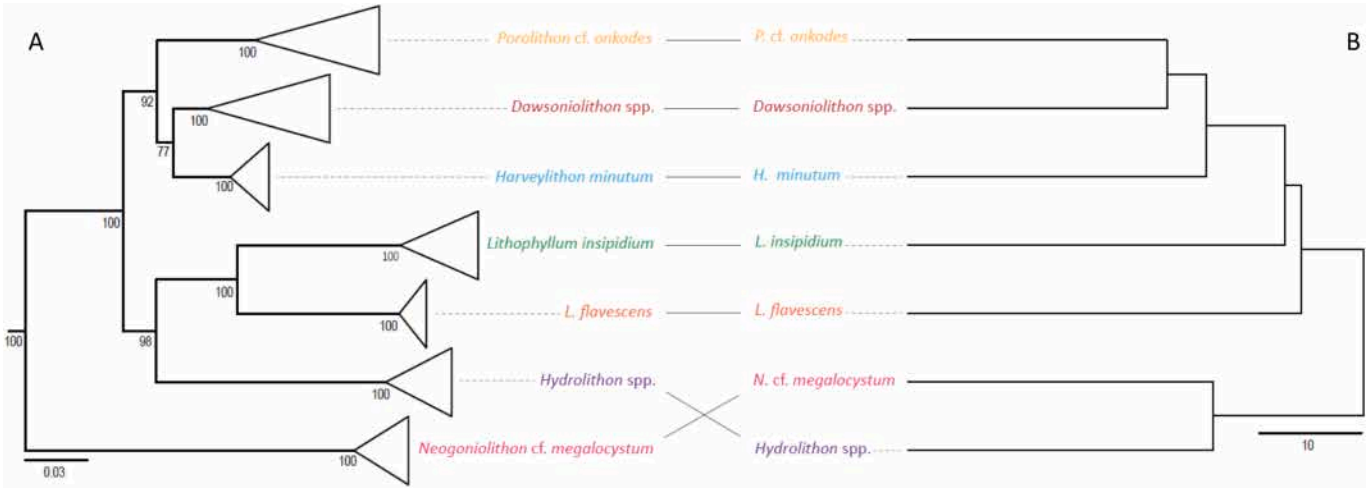

Fig. 3. (A) Multilocus (p*sbA*, COI, SSU & LSU) maximum likelihood (ML) phylogeny of CCA samples obtained with "rapid bootstrapping and search for the best-scoring ML tree" algorithm, the GTR + I + G evolutionary model, and 1000 bootstrap (bs) iterations. Bootstraps (bs) are indicated at nodes (all are >50 %). The horizontal length of the triangles represents the number of samples, while the vertical length represents the genetic divergence between these samples. (B) Corresponding hierarchical clustering analysis (HCA) dendrogram. HCA was performed on mean chemical features per species (n = 5 per species) and constructed using Euclidean distances and Ward's minimum variance method.

the study of the CCA metabolome. Technical variability was lower than biological variability for both whole fragment and algal surface samples, demonstrating the robustness and reproducibility of the method. Results showed a phylogenetic and metabolomic link in CCA species and revealed a variability in the metabolome of certain CCA species across reef habitats and microhabitats. Together these findings demonstrate that the CCA metabolome is structured by phylogeny and environmental factors. Future studies should aim to investigate the underlying factors that contribute to metabolomic variation in CCA, especially considering their important ecological role as reef building organisms and substrates for coral recruitment. This research lays the groundwork for developing a chemical baseline of a "healthy" CCA against which to chemically assess for signs of stress or disease or altered capacity to attract corals or repulse algal competitors. It represents a starting point to further investigate the ecological roles of the CCA metabolome and its potential use as a tool to assess species and ecosystem health, which could be integrated in Ecosystem or Resilience-Based Management.

Supplementary data to this article can be found online at https://doi.org/10.1016/j.algal.2025.104146.

CRediT authorship contribution statement

Camille Vizon: Writing – review & editing, Writing – original draft, Visualization, Investigation, Formal analysis, Data curation, Conceptualization. **Laura Lagourgue:** Writing – original draft, Investigation, Formal analysis, Data curation. **Hendrikje Jorissen:** Data curation. **Delphine Raviglione:** Resources, Data curation. **Claude E. Payri:** Supervision, Project administration, Funding acquisition. **Isabelle Bonnard:** Methodology, Formal analysis, Data curation, Conceptualization. **Maggy M. Nugues:** Writing – review & editing, Writing – original draft, Supervision, Project administration, Funding acquisition, Data curation, Conceptualization.

Funding

This work was supported with by the French National Research Agency through the project CORALMATES (ANR-18-CE02-0009-01) and the CNRS (PEPS-ExoMod program). C.V. and H.J. were supported by a postdoctoral grant from the Ecole Pratique des Hautes Etudes (EPHE) and a PhD grant from the Laboratoire d'Excellence CORAIL, respectively.

Declaration of competing interest

The authors declare no competing interest.

Acknowledgements

We thank the CRIOBE station staff for their assistance in the field and laboratory. Molecular analyses were performed at the Platform du Vivant (CRESICA-IRD Nouméa). Chemical analyses were performed at the MSXM Bio2Mar platform.

Data availability

Raw data for HPLC-MS analyses were deposited in the MassIVE platform at the number MSV000097553.

References

[1] O. Fiehn, Metabolomics — the link between genotypes and phenotypes, plant, Mol. Biol. 48 (2002) 155–171, https://doi.org/10.1007/978-94-010-0448-0_11.
[2] J.G. Bundy, M.P. Davey, M.R. Viant, Environmental metabolomics: a critical review and future perspectives, Metabolomics 5 (2009) 3–21, https://doi.org/10.1007/s11306-008-0152-0.
[3] X. Duportet, R.B.M. Aggio, S. Carneiro, S.G. Villas-Bôas, The biological interpretation of metabolomic data can be misled by the extraction method used, Metabolomics 8 (2012) 410–421, https://doi.org/10.1007/s11306-011-0324-1.
[4] J. Gaubert, C.E. Payri, C. Vieira, H. Solanki, O.P. Thomas, High metabolic variation for seaweeds in response to environmental changes: a case study of the brown algae *Lobophora* in coral reefs, Sci. Rep. 9 (2019) 993, https://doi.org/10.1038/s41598-018-38177-z.
[5] A.H. Hughes, F. Magot, A.F. Tawfike, C. Rad-Menéndez, N. Thomas, L.C. Young, L. Stucchi, D. Carettoni, M.S. Stanley, R. Edrada-Ebel, K.R. Duncan, Exploring the chemical space of macro- and micro-algae using comparative metabolomics, Microorganisms 9 (2021) 311, https://doi.org/10.3390/microorganisms9020311.
[6] C. Parchemin, D. Raviglione, H. Ghosson, M.-V. Salvia, C. Goossens, P. Sasal, E. Faliex, N. Tapissier-Bontemps, Development of a multiblock metabolomics approach to explore metabolite variations of two algae of the genus *Asparagopsis* linked to interspecies and temporal factors, Algal Res. 72 (2023) 103138, https://doi.org/10.1016/j.algal.2023.103138.
[7] S.S. Hamid, M. Wakayama, T. Soga, M. Tomita, Drying and extraction effects on three edible brown seaweeds for metabolomics, J. Appl. Phycol. 30 (2018) 3335–3350, https://doi.org/10.1007/s10811-018-1614-z.
[8] D.A. Payo, J. Colo, H. Calumpong, O. de Clerck, Variability of non-polar secondary metabolites in the red alga *Portieria*, Mar. Drugs 9 (2011) 2438–2468, https://doi.org/10.3390/md9112438.
[9] S. Greff, M. Zubia, C. Payri, O.P. Thomas, T. Perez, Chemogeography of the red macroalgae *Asparagopsis*: metabolomics, bioactivity, and relation to invasiveness, Metabolomics 13 (2017) 33, https://doi.org/10.1007/s11306-017-1169-z.

[10] S. Rohde, D.J. Gochfeld, S. Ankisetty, B. Avula, P.J. Schupp, M. Slattery, Spatial variability in secondary metabolites of the indo-Pacific sponge *Stylissa massa*, J. Chem. Ecol. 38 (2012) 463–475, https://doi.org/10.1007/s10886-012-0124-8.

[11] M. Reverter, M.-A. Tribalat, T. Pérez, O.P. Thomas, Metabolome variability for two Mediterranean sponge species of the genus *Haliclona*: specificity, time, and space, Metabolomics 14 (2018) 114, https://doi.org/10.1007/s11306-018-1401-5.

[12] M.M. Reddy, C. Goossens, Y. Zhou, S. Chaib, D. Raviglione, F. Nicolè, B.C.C. Hume, D. Forcioli, S. Agostini, E. Boissin, E. Boss, C. Bowler, C. de Vargas, E. Douville, M. Flores, P. Furla, P.E. Galand, E. Gilson, F. Lombard, S. Pesant, S. Reynaud, M. B. Sullivan, S. Sunagawa, R. Troublé, R.V. Thurber, P. Wincker, D. Zoccola, C. R. Voolstra, D. Allemand, S. Planes, O.P. Thomas, B. Banaigs, Multi-omics determination of metabolome diversity in natural coral populations in the Pacific Ocean, Commun. Earth Environ. 4 (2023) 281, https://doi.org/10.1038/s43247-023-00942-y.

[13] I. Belghit, J.D. Rasinger, S. Heesch, I. Biancarosa, N. Liland, B. Torstensen, R. Waagbø, E.-J. Lock, C.G. Bruckner, In-depth metabolic profiling of marine macroalgae confirms strong biochemical differences between brown, red and green algae, Algal Res. 26 (2017) 240–249, https://doi.org/10.1016/j.algal.2017.08.001.

[14] R. Marcellin-Gros, G. Piganeau, D. Stien, Metabolomic insights into marine phytoplankton diversity, Mar. Drugs 18 (2020) 78, https://doi.org/10.3390/md18020078.

[15] S.S. Hamid, M. Wakayama, K. Ichihara, K. Sakurai, Y. Ashino, R. Kadowaki, T. Soga, M. Tomita, Metabolome profiling of various seaweed species discriminates between brown, red, and green algae, Planta 249 (2019) 1921–1947, https://doi.org/10.1007/s00425-019-03134-1.

[16] C. Dell, M. Hay, Induced defence to grazing by vertebrate herbivores: uncommon or under-investigated? Mar. Ecol. Prog. Ser. 561 (2016) 137–145, https://doi.org/10.3354/meps11928.

[17] J. Wright, R. de Nys, P. Steinberg, Geographic variation in halogenated furanones from the red alga *Delisea pulchra* and associated herbivores and epiphytes, Mar. Ecol. Prog. Ser. 207 (2000) 227–241, https://doi.org/10.3354/meps207227.

[18] L.K. Polo, M.R.L. Felix, M. Kreusch, D.T. Pereira, G.B. Costa, C. Simioni, R. De P. Martins, A. Latini, E.S.I. Floh, F. Chow, F. Ramlov, M. Maraschin, Z.L. Bouzon, É. C. Schmidt, Metabolic profile of the brown macroalga *Sargassum cymosum* (Phaeophyceae, Fucales) under laboratory UV radiation and salinity conditions, J. Appl. Phycol. 27 (2015) 887–899, https://doi.org/10.1007/s10811-014-0381-8.

[19] G. Cronin, M.E. Hay, Effects of light and nutrient availability on the growth, secondary chemistry, and resistance to herbivory of two brown seaweeds, Oikos 77 (1996) 93, https://doi.org/10.2307/3545589.

[20] H. Jorissen, P.E. Galand, I. Bonnard, S. Meiling, D. Raviglione, A.-L. Meistertzheim, L. Hédouin, B. Banaigs, C.E. Payri, M.M. Nugues, Coral larval settlement preferences linked to crustose coralline algae with distinct chemical and microbial signatures, Sci. Rep. 11 (2021) 14610, https://doi.org/10.1038/s41598-021-94096-6.

[21] J. Gaubert, S. Greff, O.P. Thomas, C.E. Payri, Metabolomic variability of four macroalgal species of the genus *Lobophora* using diverse approaches, Phytochemistry 162 (2019) 165–172, https://doi.org/10.1016/j.phytochem.2019.03.002.

[22] R.S. Steneck, The ecology of coralline algal crusts: convergent patterns and adaptative strategies, Annu. Rev. Ecol. Syst. 17 (1986) 273–303.

[23] N. Schubert, K.M. Shoenrock, J. Aguirre, N.A. Kamenos, J. Silva, P.A. Horta, L. C. Hofman, Editorial: coralline algae: globally distributed ecosystem engineers, Front. Mar. Sci. 7 (2020) 352, https://doi.org/10.3389/fmars.2020.00352.

[24] C.E. Cornwall, J. Carlot, O. Branson, T.A. Courtney, B.P. Harvey, C.T. Perry, A. J. Andersson, G. Diaz-Pulido, M.D. Johnson, E. Kennedy, E.C. Krieger, J. Mallela, S. J. McCoy, M.M. Nugues, E. Quinter, C.L. Ross, E. Ryan, V. Saderne, S. Comeau, Crustose coralline algae can contribute more than corals to coral reef carbonate production, Commun. Earth Environ. 4 (2023) 105, https://doi.org/10.1038/s43247-023-00766-w.

[25] L. Harrington, K. Fabricius, G. De'ath, A. Negri, Recognition and selection of settlement substrata determine post-settlement survival in corals, Ecology 85 (2004) 3428–3437, https://doi.org/10.1890/04-0298.

[26] M. Vermeij, M. Dailer, C. Smith, Crustose coralline algae can suppress macroalgal growth and recruitment on Hawaiian coral reefs, Mar. Ecol. Prog. Ser. 422 (2011) 1–7, https://doi.org/10.3354/meps08964.

[27] C. Hochart, H. Rouzé, B. Rivière, H.-J. Ruscheweyh, L. Hédouin, X. Pochon, R. S. Steneck, J. Poulain, C. Belser, M.M. Nugues, P.E. Galand, High diversity of crustose coralline algae microbiomes across species and islands, and implications for coral recruits, Environ. Microbiome. 19 (2024) 112, https://doi.org/10.1186/s40793-024-00640-y.

[28] L. Wegley Kelly, C.E. Nelson, D. Petras, I. Koester, Z.A. Quinlan, M.G.I. Arts, L.-F. Nothias, J. Comstock, B.M. White, E.C. Hopmans, F.C. van Duyl, C.A. Carlson, L. I. Aluwihare, P.C. Dorrestein, A.F. Haas, Distinguishing the molecular diversity, nutrient content, and energetic potential of exometabolomes produced by macroalgae and reef-building corals, Proc. Natl. Acad. Sci. USA 119 (2022) e2110283119, https://doi.org/10.1073/pnas.2110283119.

[29] M.-J. Kim, J.-S. Choi, S.-E. Kang, J.-Y. Cho, H.-J. Jin, B.-S. Chun, Y.-K. Hong, Multiple allelopathic activity of the crustose coralline alga *Lithophyllum yessoense* against settlement and germination of seaweed spores, J. Appl. Phycol. 16 (2004) 175–179, https://doi.org/10.1023/B:JAPH.0000048497.62774.38.

[30] H. Mannochio-Russo, S.O.I. Swift, K.K. Nakayama, C.B. Wall, E.C. Gentry, M. Panitchpakdi, A.M. Caraballo-Rodriguez, A.T. Aron, D. Petras, K. Dorrestein, T. K. Dorrestein, T.M. Williams, E.M. Nalley, N.T. Altman-Kurosaki, M. Martinelli, J. Y. Kuwabara, J.L. Darcy, V.S. Bolzani, L. Wegley Kelly, C. Mora, J.Y. Yew, A. S. Amend, M. McFall-Ngai, N.A. Hynson, P.C. Dorrestein, C.E. Nelson, Microbiomes and metabolomes of dominant coral reef primary producers illustrate a potential role for immunolipids in marine symbioses, Commun. Biol. 6 (2023) 896, https://doi.org/10.1038/s42003-023-05230-1.

[31] T.C. Adam, D.E. Burkepile, S.J. Holbrook, R.C. Carpenter, J. Claudet, C. Loiseau, L. Thiault, A.J. Brooks, L. Washburn, R.J. Schmitt, Landscape-scale patterns of nutrient enrichment in a coral reef ecosystem: implications for coral to algae phase shifts, Ecol. Appl. 31 (2021) e2227, https://doi.org/10.1002/eap.2227.

[32] C.E. Dubé, M. Ziegler, A. Mercière, E. Boissin, S. Planes, C.A.-F. Bourmaud, C. R. Voolstra, Naturally occurring fire coral clones demonstrate a genetic and environmental basis of microbiome composition, Nat. Commun. 12 (2021) 6402, https://doi.org/10.1038/s41467-021-26543-x.

[33] H. Jorissen, C. Baumgartner, R.S. Steneck, M.M. Nugues, Contrasting effects of crustose coralline algae from exposed and subcryptic habitats on coral recruits, Coral Reefs 39 (2020) 1767–1778, https://doi.org/10.1007/s00338-020-02002-9.

[34] C. Vizon, L. Lagourgue, C.E. Payri, M.M. Nugues, Seasonal growth and calcification of three species of crustose coralline algae in Moorea, French Polynesia, Mar. Ecol. Prog. Ser. 739 (2024) 31–48, https://doi.org/10.3354/meps14626.

[35] A. Caragnano, A. Foetisch, G.W. Maneveldt, L. Millet, L. Liu, S. Lin, G. Rodondi, C. E. Payri, Revision of Corallinaceae (Corallinales, Rhodophyta): recognizing *Dawsoniolithon* gen. nov., *Parvicellularium* gen. nov. and Chamberlainoideae subfam. nov. containing *Chamberlainium* gen. nov. and *Pneophyllum*, J. Phycol. 54 (2018) 391–409. doi:https://doi.org/10.1111/jpy.12644.

[36] C. Maisl, M. Doppler, B. Seidl, C. Bueschl, R. Schuhmacher, Untargeted plant metabolomics: evaluation of lyophilization as a sample preparation technique, Metabolites 13 (2023) 686, https://doi.org/10.3390/metabo13060686.

[37] F. Giacomoni, G. Le Corguillé, M. Monsoor, M. Landi, P. Pericard, M. Pétéra, C. Duperier, M. Tremblay-Franco, J.-F. Martin, D. Jacob, S. Goulitquer, E. A. Thévenot, C. Caron, Workflow4Metabolomics: a collaborative research infrastructure for computational metabolomics, Bioinformatics 31 (2015) 1493–1495, https://doi.org/10.1093/bioinformatics/btu813.

[38] Z. Pang, J. Chong, G. Zhou, D.A. de Lima Morais, L. Chang, M. Barrette, C. Gauthier, P.-É. Jacques, S. Li, J. Xia, MetaboAnalyst 5.0: narrowing the gap between raw spectra and functional insights, Nucleic Acids Res. 49 (2021) W388–W396, https://doi.org/10.1093/nar/gkab382.

[39] H. Wickham, ggplot2: Elegant Graphics for Data Analysis, Springer New York, New York, NY, 2009. doi:https://doi.org/10.1007/978-0-387-98141-3.

[40] J. Oksanen, Package 'vegan,' (2016). https://github.com/vegandevs/vegan.

[41] P. Martinez Arbizu, pairwiseAdonis: pairwise multilevel comparison using adonis, R package version 0 (2020) 4.

[42] M. Kearse, R. Moir, A. Wilson, S. Stones-Havas, M. Cheung, S. Sturrock, S. Buxton, A. Cooper, S. Markowitz, C. Duran, T. Thierer, B. Ashton, P. Meintjes, A. Drummond, Geneious basic: an integrated and extendable desktop software platform for the organization and analysis of sequence data, Bioinformatics 28 (2012) 1647–1649, https://doi.org/10.1093/bioinformatics/bts199.

[43] NCBI (National Center for biotechnology information), Basic Local Alignment Search Tool. National Library of Medicine (US), National Center for Biotechnology Information, Bethesda, MD. https: //www.ncbi (web archive link, 16 September 2024). nlm.nih.gov/ (accessed 16 September 2024), (1988).

[44] A. Stamatakis, RAxML version 8: a tool for phylogenetic analysis and post-analysis of large phylogenies, Bioinformatics 30 (2014) 1312–1313, https://doi.org/10.1093/bioinformatics/btu033.

[45] M.A. Miller, W. Pfeiffer, T. Schwartz, Creating the CIPRES Science Gateway for inference of large phylogenetic trees, in: 2010 Gateway computing environments workshop (GCE), IEEE, New Orleans, LA, USA, 2010: pp. 1–8. doi:https://doi.org/10.1109/GCE.2010.5676129.

[46] A. Stamatakis, P. Hoover, J. Rougemont, A rapid bootstrap algorithm for the RAxML web servers, Syst. Biol. 57 (2008) 758–771, https://doi.org/10.1080/10635150802429642.

[47] A. Rambaut, Figtree v 1.4.0. http://tree.bio.ed.ac.uk/software/figtree.,(2014).

[48] S. Egan, T. Harder, C. Burke, P. Steinberg, S. Kjelleberg, T. Thomas, The seaweed holobiont: understanding seaweed–bacteria interactions, FEMS Microbiol. Rev. 37 (2013) 462–476, https://doi.org/10.1111/1574-6976.12011.

[49] M. Saha, S.M. Dittami, C.X. Chan, J. Raina, W. Stock, F. Ghaderiardakani, A.M. Valathuparambil Baby John, S. Corr, G. Schleyer, J. Todd, U. Cardini, M. M. Bengtsson, S. Prado, D. Skillings, E.C. Sonnenschein, A.H. Engelen, G. Wang, T. Wichard, J. Brodie, C. Leblanc, S. Egan, Progress and future directions for seaweed holobiont research, New Phytol. 244 (2024) 364–376, https://doi.org/10.1111/nph.20018.

[50] J.M. Sneed, R. Ritson-Williams, V.J. Paul, Crustose coralline algal species host distinct bacterial assemblages on their surfaces, ISME J. 9 (2015) 2527–2536, https://doi.org/10.1038/ismej.2015.67.

[51] N. Siboni, D. Abrego, E. Puill-Stephan, W.L. King, D.G. Bourne, J.-B. Raina, J. R. Seymour, T. Harder, Crustose coralline algae that promote coral larval settlement harbor distinct surface bacterial communities, Coral Reefs 39 (2020) 1703–1713, https://doi.org/10.1007/s00338-020-01997-5.

[52] A. Tribollet, C. Payri, Bioerosion of the coralline alga *Hydrolithon onkodes* by microborers in the coral reefs of Moorea, French Polynesia, Oceanol. Acta 24 (2001) 329–342, https://doi.org/10.1016/S0399-1784(01)01150-1.

[53] L. Behrendt, A.W.D. Larkum, A. Norman, K. Qvortrup, M. Chen, P. Ralph, S. J. Sørensen, E. Trampe, M. Kühl, Endolithic chlorophyll *d* -containing phototrophs, ISME J. 5 (2011) 1072–1076, https://doi.org/10.1038/ismej.2010.195.

[54] E.A. Zelentsova, L.V. Yanshole, Y.P. Tsentalovich, K.A. Sharshov, V.V. Yanshole, The application of quantitative metabolomics for the taxonomic differentiation of birds, Biology 11 (2022) 1089, https://doi.org/10.3390/biology11071089.

[55] J. Chervin, T. Talou, M. Audonnet, B. Dumas, L. Camborde, M.-T. Esquerré-Tugayé, C. Roux, G. Cabanac, G. Marti, Deciphering the phylogeny of violets based on

multiplexed genetic and metabolomic approaches, Phytochemistry 163 (2019) 99–110, https://doi.org/10.1016/j.phytochem.2019.04.001.

[56] R.S. Steneck, Crustose corallines, other algal functional groups, herbivores and sediments: complex interactions along reef productivity gradients., Proc. 8th Int. Coral Reef Symp. 1 (1997) 695–700.

[57] R.A. Quinn, M.J.A. Vermeij, A.C. Hartmann, I. Galtier d'Auriac, S. Benler, A. Haas, S.D. Quistad, Y.W. Lim, M. Little, S. Sandin, J.E. Smith, P.C. Dorrestein, F. Rohwer, Metabolomics of reef benthic interactions reveals a bioactive lipid involved in coral defence, Proc. R. Soc. B 283 (2016) 20160469, https://doi.org/10.1098/rspb.2016.0469.